Modulation of the Convectively Coupled Kelvin Waves by the MJO over different domains

J.M. Neena[1], E. Suhas[2], and Xianan Jiang[3]

[1]Indian Institute of Science Education and Research Pune, India
[2]Indian Institute of Science Education and Research
[3]JIFFRESSE, University of California Los Angeles, California, USA

November 21, 2022

Abstract

In this study we have examined the modulation of convectively coupled Kelvin waves (CCKW) by different Madden-Julian oscillation (MJO) states over the Indian, Pacific and Atlantic Ocean domains. Convectively active CCKW events associated with the MJO convectively active, convection suppressed and weak amplitude states were derived using wavenumber-frequency filtered outgoing long wave radiation (OLR) indices over the three domains. Composite analysis of CCKW events during different MJO states indicate that the amplitude and phase speed of CCKW are modulated by the MJO state. The amplitude of CCKW are stronger (weaker) and it propagates slower(faster) and more (less) eastward when the MJO amplitude is strong. The phase speed of CCKW is much slower over the Indian Ocean domain, while it propagates relatively faster over the Atlantic Ocean domain. It is hypothesized that the observed difference in CCKW phase speeds is related to the Gross Moist Stability (GMS). The clear linear relationship observed between the GMS and CCKW phase speeds over the different domains, during different MJO states and the observed differences in CCKW vertical structures support this hypothesis. It is found that the CCKW exhibits a baroclinic vertical structure over the Indian and Pacific Ocean domains and a barotropic vertical structure over the Atlantic Ocean. Planetary-scale convection associated with the MJO reduces the static stability allowing for baroclinic modes to prevail, which in turn reduces the GMS and the effective equivalent depth, eventually slowing down the CCKW phase propagation. The results suggest that CCKW may be treated as a mixed-moisture mode.

Modulation of the Convectively Coupled Kelvin Waves by the MJO over different domains

Neena J. M.[1], E. Suhas[1] and Xianan Jiang[2]

[1]Earth and Climate Science,

Indian Institute of Science Education and Research Pune, India.

[2]JIFFRESSE, University of California Los Angeles, California, USA

Corresponding author address:

Neena Joseph Mani,

Earth and Climate Science, IISER Pune, India

E-Mail: neena@iiserpune.ac.in

Abstract

In this study we have examined the modulation of convectively coupled Kelvin waves (CCKW) by different Madden-Julian oscillation (MJO) states over the Indian, Pacific and Atlantic Ocean domains. Convectively active CCKW events associated with the MJO convectively active, convection suppressed and weak amplitude states were derived using wavenumber-frequency filtered outgoing long wave radiation (OLR) indices over the three domains. Composite analysis of CCKW events during different MJO states indicate that the amplitude and phase speed of CCKW are modulated by the MJO state. The amplitude of CCKW are stronger (weaker) and it propagates slower(faster) and more (less) eastward when the MJO amplitude is strong. The phase speed of CCKW is much slower over the Indian Ocean domain, while it propagates relatively faster over the Atlantic Ocean domain. It is hypothesized that the observed difference in CCKW phase speeds is related to the Gross Moist Stability (GMS). The clear linear relationship observed between the GMS and CCKW phase speeds over the different domains, during different MJO states and the observed differences in CCKW vertical structures support this hypothesis. It is found that the CCKW exhibits a baroclinic vertical structure over the Indian and Pacific Ocean domains and a barotropic vertical structure over the Atlantic Ocean. Planetary-scale convection associated with the MJO reduces the static stability allowing for baroclinic modes to prevail, which in turn reduces the GMS and the effective equivalent depth, eventually slowing down the CCKW phase propagation. The results suggest that CCKW may be treated as a mixed-moisture mode.

1. Introduction

The Madden-Julian Oscillation (MJO) and the Convectively Coupled Kelvin waves (CCKW) are both eastward propagating disturbances observed in the convective and dynamical fields in the tropics (Madden and Julian 1972, Takayabu 1994, Wheeler and Kiladis 1999). Although the MJO and the CCKW exhibit similar dynamical properties, they are considered as distinct tropical modes. MJO is a ubiquitous slowly propagating ($\sim$5ms^{-1}) planetary scale tropical mode of variability that exhibits a 30-90-day periodicity. On the other hand, the CCKW are more equatorially confined fast propagating ($\sim$17 m/s) shorter spatial scale and higher frequency disturbances, with typical wavenumbers 3-8 and periodicity 3-20 days (Takayabu and Murakami 1991, Takayabu 1994, Dunkerton and Crum 1995, Wheeler and Kiladis 1999, Roundy 2008, Hendon and Wheeler 2008). They respectively account for the first and second largest variances associated with propagating disturbances in the tropics and together represent a significant fraction of tropical convection (Wheeler and Kiladis 1999, Kiladis et al. 2009). It is well known that a large fraction of tropical convection is organized by the MJO and the CCKW (Hendon and Wheeler 2008, Takayabu et al. 2016). While both the modes are active throughout the tropics, convective activity associated with the MJO are more pronounced over the Indian Ocean and the west Pacific (Hendon and Liebman 1994), and the CCKW activity is more prominent over the Inter Tropical Convergence Zone (ITCZ) (Kiladis et al. 2009, Straub and Kiladis 2002, Dias and Pauluis 2011). A crucial dynamical factor that separates the MJO from the CCKW is the amplitude of the meridional wind anomalies associated with these disturbances. Meridional winds associated with the CCKW are significantly weaker than those associated with the MJO. Seasonality is another factor that differentiates the MJO and the CCKW. While the MJO exhibits pronounced activity during boreal winter, the CCKW shows dominant activity during boreal spring (Wheeler and Kiladis 1999, Wheeler et al. 2000, Roundy and Frank 2004, Masunaga 2007).

Though their dominant spectral variances in the wavenumber-frequency space clearly indicate that the MJO and the CCKW are distinct modes, studies have reported that they are dynamically interactive (Dunkerton and Crum 2005, Straub and Kiladis 2003, Roundy 2008). Several studies have also pointed out that the MJO modulates the CCKW activity over different geographical domains (Dunkerton and Crum 1995, Straub and Kiladis 2003, Roundy 2008, Wang

and Fu 2007, Mekonnen et al. 2008, Roundy 2012, Guo et al. 2014, 2015). Several studies, mostly focusing on the western hemisphere, have reported that the CCKWs influence the synoptic and meso-scale variability over the east Pacific, Amazonia, tropical Atlantic and equatorial Africa (Kiladis et al. 2009, Nguyen and Duvel 2008, Mounier et al. 2007). Ventrice et al. (2012) suggested that the residue of MJO convective activity over the East Pacific initiates CCKWs which propagates to the tropical Atlantic and Africa. Guo et al. (2014) reported an enhanced CCKW activity when the MJO was in phases 8, 1 and 2 of the Real-time Monitoring MJO (RMM) index. Roundy (2008) explored the role of MJO convective activity in modulating the dynamical properties of CCKWs over the Indian Ocean domain, and reported that the amplitude of CCKW convective phase was higher during the convective active phase of MJO. The same study also revealed that the CCKW propagates relatively slower during MJO convectively active phase implying a stronger convection-circulation feedback.

While these studies have helped to bring out some important aspects of the MJO-CCKW interactions, some critical concerns call for a re-examination of these interactions over different geographical domains. Synoptic and meso-scale activity within the MJO convective envelop is found to be enhanced during the MJO convective active state as compared to the suppressed state (Hendon and Liebmann 1994, Dunkerton and Crum 1995). Similarly, the CCKW, during its convective active state is known to modulate the Atlantic ITCZ, West African monsoon and the mesoscale convective activity over central and eastern Africa (Liebmann et al. 2009, Wang and Fu 2007, Mournier et al. 2007, Mekonnen et al. 2008). Hence it is important to distinguish the convectively active and suppressed states of the MJO and the CCKW while examining the MJO-CCKW interactions. Studies like Ventrice et al. 2012 and Guo et al. 2014 explored the MJO-CCKW interactions by defining the MJO events based on the RMM amplitude and phase and not really separating the convectively active or suppressed state of MJO. Also, the RMM index is known to give a higher weightage to MJO circulation, especially over the western hemisphere (Ventrice et al. 2013) and hence a higher RMM amplitude may not be a sufficient criterion to define an MJO convective event.

In this study we investigate the composite structure and dynamical properties of the CCKW during different MJO states over different geographical domains by adopting an approach similar

to Dunkerton and Crum (1995) and Roundy (2008). While Roundy (2008) provided a good analysis of the MJO-CCKW interactions over the Indian ocean domain, the rather broad spectral range used for defining the MJO (wavenumbers 0 to 10, period 30 to 100 days) and CCKW (wavenumbers 1 to 14, period 2.5 to 20 days) in the study raises a concern that the CCKW convective signal separation might have been affected by the inclusion of unrelated spatial scales. Many previous studies have shown that a major fraction of the MJO convective variance falls in the scale represented by eastward wavenumbers 1-6 (Salby and Hendon 1994, Wheeler and Kiladis 1999). By using a more restrictive convective measure of the MJO and CCKW, we focus our attention on how the convectively active state of the CCKW is modulated by the MJO during its convectively active and suppressed states and when the MJO amplitude is weak.

Being a planetary scale envelop, MJO has the potential to modulate the CCKW and thereby exert a control on the other high frequency disturbances. For example, studies have reported a strong link between the passage of CCKWs and tropical cyclogenesis over different ocean basins (Bessafi and Wheeler 2006, Schreck 2015, Ventrice et al. 2012). The MJO plays an active role in this interaction by inducing significant anomalies in the CCKW meridional wind fields, which in turn can result in cyclonic rotational anomalies that can favor tropical cyclogenesis (Roundy 2008, Schreck 2015). Therefore, it is expected that a comprehensive understanding of the role of MJO phases in modulating the convective state of CCKW might provide new insights on the scale interactions between the planetary and synoptic scale disturbances which in turn might be helpful in improving the extended range prediction skill associated with these convective systems.

2. Data and Methodology

National Oceanic and Atmospheric Administration (NOAA) daily OLR data of 2.5° horizontal resolution from 1 January 1979 to 31 December 2019 was used for characterizing the convective fields of MJO and CCKW (Liebmann and Smith 1996). ERA-Interim reanalysis 2.5° horizontal resolution zonal and meridional winds, geopotential height, vertical pressure velocity, temperature and water vapor mixing ratio data at 29 pressure levels from 1000 hPa to 50 hPa from 1 January 1979 to 31 August 2019 were used to characterize the dynamic and thermodynamic fields of MJO and CCKW (Dee et al. 2011). Daily climatological seasonal cycle was estimated

by keeping the annual mean and first three harmonics of daily climatology. Daily anomalies were obtained by removing the daily climatological seasonal cycle from the raw data. The 3-20 day anomalies of dynamical and convective fields were constructed by applying the Lanczos bandpass filter on the daily anomalies (Duchon 1979).

The symmetric wavenumber-frequency power spectra (Wheeler and Kiladis 1999) of OLR normalized by the red background was used to identify and isolate the zonally propagating tropical disturbances (Figure 1a). The clear spectral gap between the MJO (wavenumber 1 to 5, period 30 to 90 day) and the CCKW (wavenumber 2 to 10, period 3 to 20 day) indicates that the two are distinct eastward propagating modes. However, Roundy (2012) cautioned that the observed spectral gap might be an artifact of the adhoc red background spectra. Figure 1b shows the wavenumber-frequency symmetric coherence squared spectra between OLR and zonal wind anomalies at 850 hPa with the phase difference between the two fields embedded on top of it as vectors. Coherence squared spectra is a useful metric that quantifies the relationship between convection and circulation in the wavenumber-frequency space (Hendon and Wheeler 2008, King et al. 2015). The coherence squared spectra is not normalized with the adhoc red background and the similar distribution of coherence squared values as in the normalized symmetric spectra (Figure 1), gives further confirmation that the MJO and the CCKW are distinct modes. It can be deduced from Figure 1b that more than 40% of CCKW circulation variability is associated with convection. It is clear from Figure 1 that majority of the CCKW variance lies between equivalent depths 10m and 100 m. The dispersion relation corresponding to equivalent depth 35 m passes through the center of local maxima of CCKW variance and from this the global average phase speed of CCKW was estimated as ~18.5 m/s, which agrees well with those reported in earlier studies (Wheeler and Kiladis 1999, Straub and Kiladis 2002). The MJO signal in OLR was extracted by applying wavenumber-frequency filter for eastward wavenumbers 1 to 6, and frequency 1/90 to 1/30 cycles/day (Figure 1). Similarly, the CCKW signal in OLR was extracted by applying a wavenumber-frequency filter for eastward wavenumbers 2 to 10 and frequency 1/20 to 1/3 cycles/day that lies between equivalent depths 10m and 100m. The additional equivalent depth criterion was applied to filter out the disturbances that fall outside the CCKW category and hence enhance the signal-to-noise ratio (Figure 1). A more restrictive OLR based measure of MJO and

CCKW activity was used since we are interested in understanding how the planetary scale MJO convective envelop modulates the CCKWs. To identify the geographical domains of activity of the MJO and the CCKW, the variance of these modes was calculated at each grid point for the period 1979-2019 (Figure 2). The MJO is dominant over the Indian Ocean, western Pacific, eastern Pacific, and equatorial Africa, whereas the CCKW is found to be active throughout the equatorial region and as expected from theory, it is more meridionally confined (Matsuno 1966). To explore how the different states of MJO (convectively active, convection suppressed, and weak amplitude) modulate the CCKW over different geographical domains, regional indices representing the MJO and the CCKW were constructed by area averaging the MJO and CCKW filtered OLR anomalies over the three domains and then normalizing the resultant time series with their respective standard deviations. The MJO and CCKW filtered OLR anomalies were area averaged over $10° \times 10°$ grid boxes over the Indian Ocean (5°S-5°N, 75°E-85°E), Pacific Ocean (5°S-5°N, 170°E-180°E) and equatorial Africa (5°S-5°N, 0°-10°E). The grid boxes were identified as regions where both the modes were active, and the results presented in the study are not very sensitive to the choice of the grid boxes.

The indices are designed to capture the passage of MJO and CCKW over the three domains. CCKW convective events that pass over a given domain are identified as when the OLR-based regional CCKW index is less than -1.0 at least for three consecutive days. The peak of each event is then identified as the local minima. To examine the dependence of the CCKW convectively active state on the different MJO states, the CCKW events are further grouped as co-occurring with MJO convectively active, convection suppressed and weak amplitude states. A CCKW event is grouped into the MJO convectively active category if the MJO index is less than -1.0 throughout the length of the CCKW event. Similarly, if the MJO index is greater than 1.0 throughout the length of a CCKW event, the CCKW event is then categorized as co-occurring with MJO convection suppressed state. A CCKW event is grouped into the MJO weak amplitude category if the MJO index lies between -0.5 and 0.5 throughout the event length.

A Radon Transform Method (RTM) was used for objectively estimating the phase speeds of CCKW from the time-longitude distribution of OLR anomalies during the CCKW events (Challenor et al. 2001). RTM is known to be less sensitive to the outliers than fitting a line and

hence many recent studies have used this technique to estimate the phase speeds of propagating disturbances (Challenor et al. 2001, Yang et al. 2007, Dias and Pauluis 2011, Mayta et al. 2021). Refer to Yang et. al. (2007) for more details on RTM.

The normalized gross moist stability (GMS) is calculated following Benedict et al. (2014) and Jiang et al. (2015) methodology. The total GMS and its vertical and horizontal components are represented as follows.

$$\Gamma = -\frac{T_R\left([\vec{v}.\nabla s]+\left[\omega\frac{\partial s}{\partial p}\right]\right)}{L(\nabla.(r\vec{v}))} \quad \text{----------} \quad (1)$$

$$\Gamma_v = -\frac{T_R\left(\left[\omega\frac{\partial s}{\partial p}\right]\right)}{L(\nabla.(r\vec{v}))} \quad \text{----------------} (2)$$

$$\Gamma_h = -\frac{T_R([\vec{v}.\nabla s])}{L(\nabla.(r\vec{v}))} \quad \text{----------------} \quad (3)$$

Where Γ is the total GMS, Γ_v and Γ_h are the vertical and horizontal components of GMS respectively, T_R is the reference temperature (273.15 K), L is the latent heat of vaporization (2.5×10^6 Jkg^{-1}), r is the water vapor mixing ratio, ω is the vertical pressure velocity, $\vec{v}$ is the horizontal wind vector and s is the moist entropy. The square brackets represent the mass-weighted vertical integral from 1000 hPa to 100 hPa. Refer to Benedict et al. (2014) and Jiang et al. (2015) for more details about GMS computations.

3. Results and Discussions

The CCKW event statistics collected over the three domains are summarized in Table 1. Among the three domains, the highest number of CCKW events are observed over the Pacific Ocean domain and the number of CCKW events observed over the Indian and Atlantic Ocean domains are comparable. The observation of large number of CCKW events over the Pacific Ocean is consistent with the geographical distribution of CCKW variance (Figure 2b). The relatively small number of CCKW events observed during different MJO states is possibly due to the differences in seasonality of the MJO and CCKW. It is noted that the MJO becomes more active during boreal winter and the CCKW is found to be more active during May-June months (Wheeler and Kiladis 1999, Roundy and Frank 2004, Masunaga 2007). It is interesting to note that about 42% of the CCKW events over the Pacific Ocean domain occurred when the MJO amplitude was

weak. About 21% of the CCKW events occurred along with strong amplitude MJO, of which, a higher number of events were associated with the MJO convective active state (14%), as compared to the MJO convection suppressed state (7%). Over the other two domains, about 36-38% of the CCKW events occurred when the MJO amplitude was strong and about 28-30% of the CCKW events occurred when the MJO amplitude was weak. Similar to the Pacific, the CCKW events over the Atlantic show a greater preference for the MJO convective active state (23%), as compared to the MJO convection suppressed state (16%). Over the Indian Ocean, about 17% CCKW events are associated with MJO convective active state and about 19% CCKW events are associated with MJO convection suppressed state.

Figure 3 shows the composites constructed using unfiltered OLR and wind anomalies for the peak days of all CCKW events associated with different MJO states over the three domains. The convectively active phase of CCKW over each domain, highlighted by the overlaid contours, is constructed by compositing the CCKW filtered negative OLR anomalies over the peak days of all CCKW events during the different MJO states. The unfiltered OLR and wind anomaly composites are mostly dominated by the MJO structure during the convectively active state of MJO (Figure 3a), while the CCKW structure is discernible in the unfiltered OLR and wind anomaly composites during MJO weak amplitude states (Figure 3c). Hence the methodology employed for identifying the CCKW events and MJO states seems to be robust enough to capture the CCKW structures.

The mean spatio-temporal structure and evolution of the CCKW events during MJO convectively active, convection suppressed and weak amplitude states were examined by carrying out a lead-lag composite analysis over the three domains. Since the unfiltered anomalies are dominated by the MJO, 3-20 day bandpass filtered OLR and wind anomalies were used for characterizing the evolution of the dynamic and convective fields associated with the CCKW. As the event identification is already based on wavenumber-frequency filtered OLR anomalies, to avoid over-smoothing we refrained from using wavenumber-frequency filtered OLR anomalies for constructing the composites. Roundy (2015) pointed out the significance of the smaller spatial scale CCKW and by using only time filtered anomalies in the composite analysis, we try to preserve the smaller spatial scale CCKW. The composite structure of CCKW was extracted for

different leads, 4 days before and 4 days after the peak of the CCKW events. Lead-lag composites of CCKW events that occurred during the MJO convectively active, convection suppressed and weak amplitude states were created over the three domains. Figure 4 shows the lead-lag composites of 3-20 day bandpass filtered OLR and 850 hPa wind anomalies associated with the CCKW events over the Indian Ocean domain that co-occurred with different MJO states. The eastward propagation of CCKW from eastern Indian Ocean to the Maritime continent is evident, and as reported in many previous studies, westerly (easterly) wind anomalies are found to be associated with enhanced (suppressed) convection of CCKW (Wheeler and Kiladis 1999, Wheeler et al. 2000, Roundy and Frank 20004). The amplitude and meridional extent of the CCKW convective anomalies is largest when it occurs during MJO convectively active state. The rotational component of CCKW wind is more predominant, with a stronger meridional component when the MJO amplitude is strong (Figure 4b, 4g). From the lead-lag composites, it can be inferred that the average periodicity of CCKW events over the Indian Ocean domain is about 10 days. The eastward propagation of CCKW events from west Pacific to east Pacific is evident in the lead-lag composites of CCKW events over the Pacific Ocean domain during different MJO states (Figure 5). It is interesting to note that the CCKW convection shows more eastward extent when the MJO amplitude is strong. As observed over the Indian Ocean domain, CCKW wind components are more zonally oriented when the MJO amplitude is weak. CCKW over the Pacific Ocean domain exhibits a dominant spatial scale of wavenumber 4 and a period of 6-7 days (Figure 5). Though the CCKW index over the Pacific Ocean domain was derived from an equatorial region, it captures the off equatorial distribution of OLR anomalies as the CCKW propagates over the eastern Pacific. Figure 6 shows the lead-lag composites of CCKW events observed over the Atlantic Ocean domain during different MJO states. It describes the propagation of CCKW from equatorial central America to the west African region. The amplitude of CCKW is higher when the MJO is in the convectively active state and irrespective of the MJO state, the CCKW events over the Atlantic Ocean exhibit a smaller spatial scale (wavenumber 5 to 6) and a shorter periodicity (5 to 7 days).

The CCKW are observed to have a baroclinic vertical structure (Kiladis et al. 2009). Roundy (2008) reported that the CCKW over the Indian Ocean domain associated with MJO convectively active state exhibit more pronounced meridional wind anomalies at 200 hPa. In order

to understand whether the vertical structure of CCKW over the three domains is modulated by the MJO state, composites of CCKW OLR and 200 hPa wind anomalies were examined for the MJO convectively active, convection suppressed and weak amplitude states (Figure 7). It is found that over all the three domains the CCKW have a significant meridional wind component when the MJO amplitude is strong. Upper level winds associated with the CCKW are more zonal when the MJO amplitude is weak. The rotational component of CCKW winds are more predominant when the MJO amplitude is strong.

The phase speed of CCKW over the three domains during different MJO states were quantified by applying RTM on the latitudinally averaged lead-lag composites of OLR and 850 hPa zonal wind anomalies. Figure 8 shows the composite time-longitude distribution of CCKW OLR and 850 hPa zonal wind anomalies averaged over 5ºS-5ºN during different MJO states over the three domains. It is evident that the CCKW amplitude is largest and it propagates beyond the Maritime continent when the MJO is convectively active (Figure 8 a-c). Objective estimation of the CCKW phase speed using RTM reveals that the CCKW convective phase propagates with an approximate phase speed of 13.37 ms^{-1} during MJO convective active state, 14.48 ms^{-1} during MJO convection suppressed state and 15.8 ms^{-1} when the MJO amplitude is weak over the Indian Ocean. The observed range of CCKW phase speed over the Indian Ocean domain largely agrees with the estimates reported by earlier studies (Dunkerton and Crum 1995, Roundy 2008), even though there were some differences in the methodology employed for identifying the CCKW and MJO events. The CCKW phase speed is relatively higher when the MJO is convectively suppressed and when the MJO amplitude is weak. Over the Pacific Ocean domain, the CCKW phase speed is faster than that over the Indian Ocean (Figure 8 d-f). CCKW phase speed during MJO convectively active state (15.78 ms^{-1}) is comparable to the phase speed during MJO convection suppressed state (15.11 ms^{-1}). The CCKW propagates with an approximate phase speed of 16.52 ms^{-1} when the MJO amplitude is weak. Compared to the other two domains, CCKW over the Atlantic domain propagates with a significantly faster speed during different MJO states (Figure 8 g-i). A phase speed of 20.27 ms^{-1} is observed when the MJO is convectively active, 22.85 m/s when the MJO convection is suppressed and 24.4 m/s when the MJO amplitude is weak. It is also observed that the CCKW amplitude is significantly higher when the MJO is convectively active. It is interesting

to note that the average CCKW phase speed ($\sim$17.6 ms^{-1}) across the different domains, during different MJO states approximately agrees with the value derived from the wavenumber-frequency spectra (18.5 ms^{-1}, Figure 1).

Convection-circulation coupling strength and gross moist stability are major factors that can affect the phase speed of MJO and other convectively coupled equatorial waves (Roundy 2008, Kiladis et al. 2009, Frierson et al. 2011, Benedict et al. 2014, Jiang et al. 2015). We investigate the relative roles of these factors in explaining the observed differences in CCKW phase speeds during different MJO states over the different domains. Roundy (2008) reasoned that a stronger feedback between convection and circulation might be one of the reasons for the slower phase speed of CCKW over the Indian Ocean during MJO convectively active state. Differences in convection-circulation coupling strength during different MJO states is evident from figure 9. The coherent eastward propagation of zonal wind anomalies and collocated OLR anomalies and the relatively slow phase speed of CCKW imply a stronger convection-circulation coupling during MJO convectively active state. Irrespective of the MJO state, the local maxima of easterly wind anomalies are often located to the east of OLR minima over all the domains. The phase vectors in the coherence squared spectra between OLR and 850hPa zonal winds (Figure 1b) also indicate the same.

In order to bring out a more clear and direct evidence for the strength of convection-circulation coupling in the CCKW time scale during different MJO states over different domains, the coherence squared spectra were calculated for a 30-day window period centered around each of the CCKW events and the resultant values were averaged between 5ºS and 5ºN latitudes. The composite coherence squared spectra was then computed over all the CCKW events that fall under the different MJO states, over the three domains (Figure 9). Larger coherence squared values indicate stronger convection-circulation coupling. The distribution of coherence squared values for different MJO states affirms the inferences deduced based on the composite analysis of CCKW events. Differences are also observed in the coherence squared distribution during strong and weak amplitude MJO states over all the three domains (Figure 9). Over the Indian Ocean domain, high coherence squared values are observed mostly between 6-15 days period. The coherence squared values are relatively weak and confined to a smaller range of longitudes when the MJO amplitude

is weak. Over the Pacific Ocean domain, stronger coherence squared values are observed when the MJO convection is suppressed. When the MJO amplitude is weak, the coherence squared values are insignificant. Over the Atlantic Ocean domain, relatively higher coherence squared values are observed when the MJO is convectively active/suppressed and the coherence squared values are small and insignificant when the MJO amplitude is weak. However, this is inconsistent with the observed higher phase speed of CCKW over the Atlantic when the MJO amplitude is high, as a stronger convection-circulation coupling would result in a slower phase speed. Significant coherence squared values are confined to a 5-8-day periodicity when the MJO is convectively suppressed and is spread across 4-15 day periodicity when the MJO is convectively active.

It has been shown that both the upper tropospheric and lower stratospheric zonal winds respond to the CCKWs (Hendon and Wheeler 2008). The coupling between CCKW convection and zonal wind anomalies at different pressure levels from 1000 hPa to 50 hPa were examined using coherence squared spectral analysis. The approach is similar to the one described above and over the three domains, for the different MJO states the composite coherence squared spectra was computed at each pressure level. Figure 10 a-c show the longitude-pressure distribution of composite coherence squared values averaged for the period 7-15 days over the Indian Ocean domain for different MJO states. Over the 60°E-100°E longitudes, a strong convection-circulation coupling is observed below the 500 hPa level, as well as near the tropopause and lower stratosphere when the MJO amplitude is strong. But, compared to the other two domains, relatively higher coherence squared values are observed in the lower troposphere over the Indian ocean domain, even when the MJO amplitude is weak. A stronger convection-circulation coupling is observed in the upper levels only when the MJO is convectively active. It is well documented that the MJO is more intense and active over the Indian Ocean domain and it might be possible that the MJO enhances the convection-circulation coupling strength in the CCKW scale through nonlinear scale interactions. The longitude-pressure distribution of composite coherence squared values averaged over the period 7-10 days over the Pacific domain is shown in Figure 10 d-f. In contrast to the other two domains, high coherence squared values are observed when MJO convection is suppressed (Figure 10 d-f). Interestingly, both in the upper and lower troposphere, when the MJO

convection is suppressed the coherence squared values are higher, implying stronger convection-circulation coupling. The coherence squared values are negligible when the MJO amplitude is weak. Over the Atlantic Ocean domain, the longitude-pressure distribution of coherence squared values were calculated by averaging the composite coherence squared values that fall between 5-10 days periodicity. Higher coherence squared values are observed in the lower and upper troposphere and in the lower stratosphere when the MJO amplitude is strong. Stronger convection-circulation coupling is observed when the MJO is convectively active. Compared to the other two domains, higher coherence between convection and circulation are observed in the upper troposphere when the MJO amplitude is strong.

Many previous studies identify the MJO and the major convectively coupled equatorial waves as moist modes and hypothesize that the phase speed of these waves may be related to the GMS (Neelin et al. 1987, Frierson et al. 2011, Benedict et al. 2014, Jiang et al. 2015). According to linear wave theory, the phase speed of equatorial waves is proportional to the square root of its equivalent depth. Since GMS is considered as a measure of effective equivalent depth, a linear relationship is expected between the magnitude of GMS and the phase speed of convectively coupled equatorial waves. However, such an association has not been examined so far using observations. Benedict et al. (2014) found a linear relationship between the GMS and eastward propagation phase speed of MJO in climate model simulations. Frierson et al. (2011) attributed the differences in CCKW phase speed simulated by different convective triggers to the differences in GMS. To explain the observed differences in CCKW phase speed over the different domains during different MJO states, we explore the possible relationship between CCKW phase speed and the corresponding magnitude of GMS.

The GMS and its vertical and horizontal components are calculated over the different domains during different MJO states and compared with the corresponding CCKW phase speeds. A strong linear relationship (correlation coefficient ~ 0.9) is observed between the vertical component of GMS and CCKW phase speeds (Figure 11). For example, highest GMS is observed when the MJO amplitude is weak over the Atlantic Ocean domain and lowest GMS is observed when the MJO is convectively active over the Indian Ocean domain. The observed relationship explains not only the differences in CCKW phase speed over the different domains but also the

differences observed during different MJO states. The possible connection between the GMS and CCKW is hypothesized as follows. Reduced static stability in the regions of planetary-scale convection allows for baroclinic modes to exist. A baroclinic vertical structure permits communication between the lower and upper troposphere resulting in a lower GMS. A lower effective equivalent depth due to the lower GMS will in turn lower the phase speed of the waves (Kiladis et al. 2009, Frierson et al. 2011).

To test this hypothesis, we examined the composite vertical structures of CCKW during different MJO states over the different domains. Because the vertical structure of CCKW is more evident in temperature (Kiladis et al. 2009, Frierson et al. 2011), the composite vertical structure is extracted using 3-20 day bandpass filtered temperature anomalies (Figure 12). CCKW over the Indian and Pacific Ocean domains exhibit a second baroclinic vertical structure with an east-west tilt in the troposphere (more vertical tilt is found over the Indian Ocean domain) and a west-east tilt in the lower stratosphere (Wheeler et al. 2000, Kiladis et al. 2009). On the other hand, the vertical structure of CCKW over the Atlantic Ocean domain is different from the other two domains. The vertical structure of CCKW over the Atlantic Ocean domain is nearly barotropic in the troposphere and exhibit a west-east tilt in the lower stratosphere. It can be inferred from figure 12 that the vertical scale of CCKW is relatively larger over the Atlantic Ocean domain and smaller over the Indian Ocean domain.

In general, the Indo-Pacific domain supports planetary-scale convection and hence baroclinic vertical structures are favored over the region. The relative strength of MJO is different over different domains (Figure 2, Table 1), with strongest amplitude observed over the Indian Ocean domain and weakest amplitude observed over the Atlantic Ocean domain. Stronger planetary-scale convection associated with the MJO might make the Indian and Pacific Ocean domains more baroclinic, reduce the GMS and lower the CCKW phase speeds. On the other hand, the relative strength of MJO being small over the Atlantic Ocean domain might result in weak baroclinic modes and favor a higher GMS which is reflected in the overall higher CCKW phase speeds. It is clear from Figure 12 that the observed vertical structure of CCKW in the troposphere over the Atlantic Ocean domain is nearly barotropic. The observed differences in CCKW vertical structures over the different domains are consistent with the observed differences in GMS and

phase speeds, in accordance with the hypothesis. The relationship between GMS and CCKW phase speed and the range of magnitude of CCKW phase speed indicate that the CCKW might be a mixed moisture mode (Ademes et al. 2019).

4. Summary and Conclusions

We have examined the modulation of convective activity associated with the CCKW by different MJO states over the Indian, Pacific and Atlantic Ocean domains using OLR and ERA-Interim reanalysis wind anomalies for the period 1979 to 2019. Dominant spatial and temporal scales of the CCKW and MJO were identified using wavenumber-frequency power spectral analysis of OLR and coherence squared spectral analysis of OLR and 850 hPa zonal wind anomalies. Convective anomalies with wavenumber 1-6 and 30-90 day period were identified as the MJO and the CCKW was defined by wavenumbers 2-10 and 3-20 day period (Figure 1). It was also observed that the CCKW spectral power falls between equivalent depths 10 and 100 m. MJO and CCKW convective signals were extracted by applying wavenumber-frequency filter on the OLR data using these criteria. Based on the spatial distribution of MJO and CCKW variance (Figure 2), three equatorial locations where both the MJO and the CCKW are active were identified over the Indian Ocean (5°S-5°N, 75°-85°E), Pacific Ocean (5°S-5°N, 170°-180°E) and Atlantic Ocean (5°S-5°N, 0°-10°E) domains. Convectively active CCKW events over the three domains were identified using CCKW filtered OLR data averaged over the respective local domains. Further, the CCKW events that occurred together with MJO convectively active, convection suppressed and weak amplitude states were identified.

Lead-lag composite analysis reveal that the strong amplitude MJO state modulate the intensity and phase speed of the CCKW events (Figure 3-5). It is also noted that over the three domains, the CCKW propagates more eastward when the MJO is convectively active. Analysis of the phase speed of the CCKW convective events over the three domains during different MJO states reveal that the CCKW propagates with a consistently faster phase speed when the MJO amplitude is weak (Figure 8). It is observed that, in general, the CCKW propagates relatively slower over the Indian Ocean domain (~13-16 ms^{-1}) and relatively faster over the Atlantic Ocean domain (~20-24 ms^{-1}). To understand the differences in CCKW phase speeds over the different

domains during different MJO states, the relationship of CCKW phase speed with the convection-circulation coupling strength and gross moist stability was explored.

Convection-circulation coupling strength during different MJO states were quantified by performing coherence squared spectral analysis between OLR and 850 hPa zonal wind anomalies for all the CCKW events observed over the three domains (Figure 9). The analysis reveals that convection-circulation coupling strength is indeed higher when the MJO amplitude is strong. Longitude-pressure distribution of coherence squared values averaged over the CCKW frequency range show that the coherence between OLR and zonal wind anomalies is significantly higher when the MJO amplitude is strong. The observation of higher coherence squared values when the MJO amplitude is strong and lower coherence squared values when the MJO amplitude is weak can be interpreted as a difference in the convection-circulation coupling strength. Strong coherence is observed in the upper troposphere and lower stratosphere when the MJO amplitude is strong implying the possible role of MJO in modulating the stratospheric circulation by influencing vertical easterly momentum transport via CCKW (Figure 10). However, convection-circulation coupling strength does not explain the differences in CCKW phase speed observed over the different domains.

On the other hand, the distribution of GMS over different domains during different MJO states exhibit a linear relationship with the CCKW phase speeds (Figure 11). A stronger relationship is observed between the vertical component of GMS and CCKW phase speed. Lowest GMS value is observed over the Indian Ocean domain when the MJO is convectively active, and highest GMS value is observed over the Atlantic Ocean domain when the MJO amplitude is weak. These observations are consistent with the CCKW phase speeds. It can be hypothesized that planetary scale convection associated with the MJO and the resulting low static stability allows for baroclinic modes to prevail, which in turn reduces the GMS and effective equivalent depth and slows down the CCKW phase speed (Kiladis et al. 2009, Frierson et al. 2011). The CCKW composite vertical structures over different domains support this hypothesis (Figure 12). While the CCKW exhibits a baroclinic vertical structure over the Indian and Pacific Ocean domains, a nearly barotropic vertical structure is observed over the Atlantic Ocean domain. The observed range of

values of CCKW phase speeds and its relationship with GMS suggest that the CCKW may be treated as a mixed-moisture mode (Adems et al. 2019).

The study explores the modulation of CCKW convective phase by the co-occurring MJO state. It should be noted that the lead-lag interactions between CCKW and MJO states are equally important. For example, CCKW is considered as one of the precursors for MJO initiation over the Indian Ocean domain, and the CCKW over the South American and Atlantic Ocean may be excited from the residue of MJO over the east Pacific (Masunaga 2007, Ventrice et al. 2012). These aspects are of great importance in terms of the predictability of the MJO as well as the synoptic and mesoscale systems and these interactions will be addressed in a future study.

Acknowledgements

Reference

Adems, A. F., D. Kim, S. K. Clark, Y. Ming, and K. Inoue 2019: Scale analysis of moist thermodynamics in a simple model and the relationship between moisture modes and gravity waves. J. Atmos. Sci., 76, 3863-3881.

Benedict, J. J., E. D. Maloney, A. H. Sobel, and D. W. Frierson 2014: Gross moist stability and MJO simulation skill in three full-physics GCMs. J. Atmos. Sci., 71, 3327-3349.

Bessafi, M., and M. C. Wheeler, 2006: Modulation of South Indian Ocean tropical cyclones by the Madden–Julian oscillation and convectively coupled equatorial waves. Mon. Wea. Rev., **134**, 638–656.

Challenor, P. G., P. Cipollini, and D. Cromwell, 2001: Use of the radon transform to examine properties of oceanic Rossby waves. J. Atmos. Oceanic Technol., 18, 1558–1566.

Dee D. P., and Coauthors, 2011: The ERA-Interim reanalysis: configuration and performance of the data assimilation system. Q.J.R. Meteorol. Soc., **137**, 553–597.

Dias, J. and O. Pauluis, 2011: Modulation of the phase speed of convectively coupled Kelvin waves by the ITCZ. J. Atmos. Sci.,68,1446-1459.

Duchon, C. E., 1979: Lanczos filter in one and two dimensions. J. Appl. Meteor., 18, 1016–1022.

Dunkerton, T. J., and F. X. Crum, 1995: Eastward propagating; 2- to 15-day equatorial convection and its relation to the tropical intraseasonal oscillation. J. Geophys. Res., 100, 25 781–25 790.

Frierson, D. M. W., D. Kim, I-S., Kang, M-I., Lee, J. Lin 2011: Structure of AGCM-simulated convectively coupled Kelvin waves and sensitive to convective parameterization. J. Atmos. Sci., 68, 26-45.

Guo, Y., Jiang, X., and Waliser, D. E., 2014: Modulation of convectively coupled Kelvin waves over south America and the tropical Atlantic Ocean with the Madden-Julian oscillation. J. Atmos. Sci., 71, 1371-1388.

Guo, Y., Waliser, D. E., and Jiang, X., 2015: A systematic relationship between the representations of convectively coupled equatorial wave activity and the Madden–Julian Oscillation in climate model Simulations, J. Climate, 28, 1881-1904.

Hendon, H. H., and B. Liebmann, 1994: Organization of convection within the Madden-Julian oscillation. J. Geophys. Res., 99, 8073-8083.

Hendon, H. H., and M. C. Wheeler, 2008: Some space-time spectral analysis of tropical convection and planetary-scale waves. J. Atmos. Sci., **65**, 2936-2948.

Jiang, X., and Coauthors, 2015: Vertical structure and physical processes of the Madden-Julian oscillation: Exploring key model physics in climate simulations. J. Geophys. Res. Atmos., 120, 4718–4748.

Kiladis, G. N., M. C. Wheeler, P. T. Haertel, K. H. Straub, and P. E. Roundy, 2009: Convectively coupled equatorial waves. Rev. Geophys., **47**, RG2003, doi:10.1029/2008RG000266.

King, M. J., M. C. Wheeler, and T. P. Lane 2015: Association of convection with the 5-day Rossby-Haurwitz wave. J. Atmos. Sci., 72, 3309-3321.

Liebmann, B. and C.A. Smith, 1996: Description of a Complete (Interpolated) Outgoing Longwave Radiation Dataset. Bulletin of the American Meteorological Society, **77**, 1275-1277.

Liebmann , B., Kiladis, G. N., L.M.V. Carvalho, C. Jones, C.S. Vera, I. Blade, and D. Allured 2009: Origin of convectively coupled Kelvin waves over south America. J. Climate, 22, 300-315.

Masunaga, H., 2007: Seasonality and regionality of the Madden- Julian oscillation, Kelvin wave, and equatorial Rossby wave. J. Atmos. Sci., **64**, 4400−4416.

Mekonnen, A., C. D. Thorncroft, A. R. Aiyyer, and G. N. Kiladis, 2008: Convectively coupled Kelvin waves over tropical Africa during the boreal summer: Structure and variability. J. Climate, 21, 6649–6667.

Mounier, F., G. N. Kiladis, and S. Janicot, 2007: Analysis of the dominant mode of convectively coupled Kelvin waves in the West African monsoon. J. Climate, 20, 1487–1503.

Matsuno, T., 1966: Quasi-geostrophic motions in the equatorial area. J. Meteor. Soc. Japan, **44**, 25–43.

Mayta, V. C., G. N. Kiladis, J. Dias, P. L. Silva Dias, and M. Gehne 2021: Convectively Coupled Kelvin Waves over Tropical South America. J. Climate, 34, 6531-6547.

Neelin, J. D., I. M. Held, and K. H. Cook, 1987: Evaporation–wind feedback and low-frequency variability in the tropical atmosphere. J. Atmos. Sci., 44, 2341–2348.

Nguyen, H., and J. P. Duvel, 2008: Synoptic wave perturbations and convective systems over equatorial Africa. J. Climate, 21, 6372–6388.

Roundy, P. E., 2008: Analysis of convectively coupled Kelvin waves in the Indian Ocean MJO. J. Atmos. Sci., 65, 1342–1359.

Roundy, P.E., 2012: Observed structure of convectively coupled waves as a function of equivalent depth: Kelvin waves and the Madden–Julian oscillation. J. Atmos. Sci., 69, 2097–2106.

Roundy, P. E., 2015: On the interpretation of EOF analysis of ENSO, atmospheric Kelvin waves, and the MJO. J. Climate, 28, 1148-1165.

Roundy, P. E., and W. M. Frank, 2004: A climatology of waves in the equatorial region. J. Atmos. Sci., **61**, 2105–2132.

Salby, M. L., and H. H. Hendon, 1994: Intraseasonal behaviour of clouds, winds, and temperature in the tropics. J. Atmos. Sci., 51, 2207-2224.

Schreck III, C. J., 2015: Kelvin waves and tropical cyclogenesis: A global survey. Mon. Wea. Rev., 143, 3996-4011.

Straub, K. H., and G. N. Kiladis, 2002: Observations of a convectively coupled Kelvin wave in the eastern Pacific ITCZ. J. Atmos. Sci., 59, 30–53.

Straub, K. H., and G. N. Kiladis, 2003: The observed structure of convectively coupled Kelvin waves: Comparison with simple models of coupled wave instability. J. Atmos. Sci., 60, 1655–1668.

Takayabu, Y. N., 1994: Large-scale cloud disturbances associated with equatorial waves. Part I: Spectral features of the cloud disturbances. J. Meteor. Soc. Japan, **72**, 433–449.

Takayabu, Y.N., and M. Murakami, 1991: The structure of super cloud clus- ters observed in 1–20 June 1986 and their relationship to easterly waves. J. Meteor. Soc. Japan, 69, 105–125.

Takayabu, Y. N., G. N. Kiladis, and V. Magaña, 2016: Michio Yanai and tropical waves, Meteorol. Monogr., **56**, 3–1.

Ventrice, M. J., C. D. Thorncroft, and C. J. Schreck III, 2012: Impacts of convectively coupled Kelvin waves on environmental conditions for Atlantic tropical cyclogenesis. Mon. Wea. Rev., 140, 2198–2214.

Ventrice, M. J., M. C. Wheeler, H. H. Hendon, C. J. Schreck III, C. D. Thorncroft, and G. N. Kiladis 2013: A modified multivariate Madden-Julian oscillation index using velocity potential. Mon. Wea. Rev., 141, 4197-4210.

Wang, H., and R. Fu, 2007: The influence of Amazon rainfall on the Atlantic ITCZ through convectively coupled Kelvin waves. J. Climate, 20, 1188–1201.

Wheeler, M., and G. N. Kiladis, 1999: Convectively coupled equatorial waves: Analysis of clouds and temperature in the wavenumber–frequency domain. J. Atmos. Sci., **56**, 374–399.

Wheeler, M., G. N. Kiladis, P. J, Webster, 2000: Large-scale dynamical fields associated with convectively coupled equatorial waves. J. Atmos. Sci., **57**, 613-640.

Yang, G-Y., B. Hoskins, and J. Slingo 2007: Convectively coupled equatorial waves. Part II: Propagation characteristics. . J. Atmos. Sci., 64, 3424-3437.

Domain	Number of MJO convectively active CCKW events	Number of MJO suppressed convection CCKW events	Number of MJO weak amplitude CCKW events	Total number of CCKW events	MJO index standard deviation (W/m²)	CCKW index standard deviation (W/m²)
IO	21	24	35	125	6.8	3.4
PO	20	10	59	141	3.9	3.7
AO	27	19	37	120	2.7	3.8

Table 1. CCKW event statistics over different domains during the period 1979-2019. IO represents Indian Ocean, PO represents Pacific Ocean and AO represents Atlantic Ocean domains.
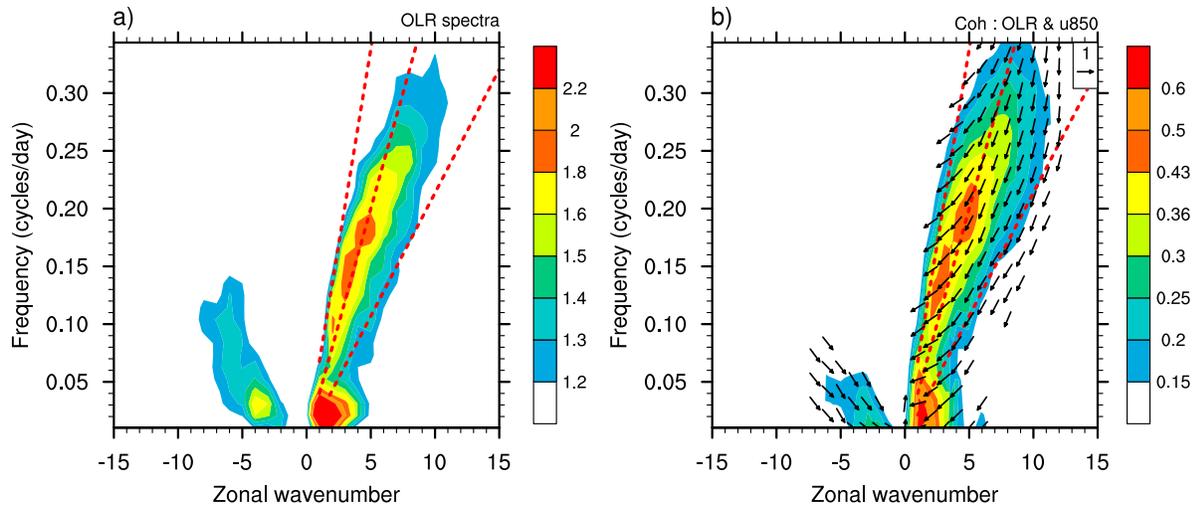
Figure 1. a) Symmetric/background wavenumber-frequency power spectra of OLR b) Symmetric wavenumber-frequency coherence squared spectra (shaded contours) and phase vectors of OLR and zonal wind at 850 hPa (u850) for the period 1979-2019. Red dashed lines represent the dispersion relation of Kelvin waves with equivalent depths 10m, 35m and 100m. Shaded regions are statistically significant at 99% confidence level. Upward (downward) directed vectors implies that OLR and u850 are in (out of) phase, and vectors directed towards right (left) implies that OLR leads (lags) u850.
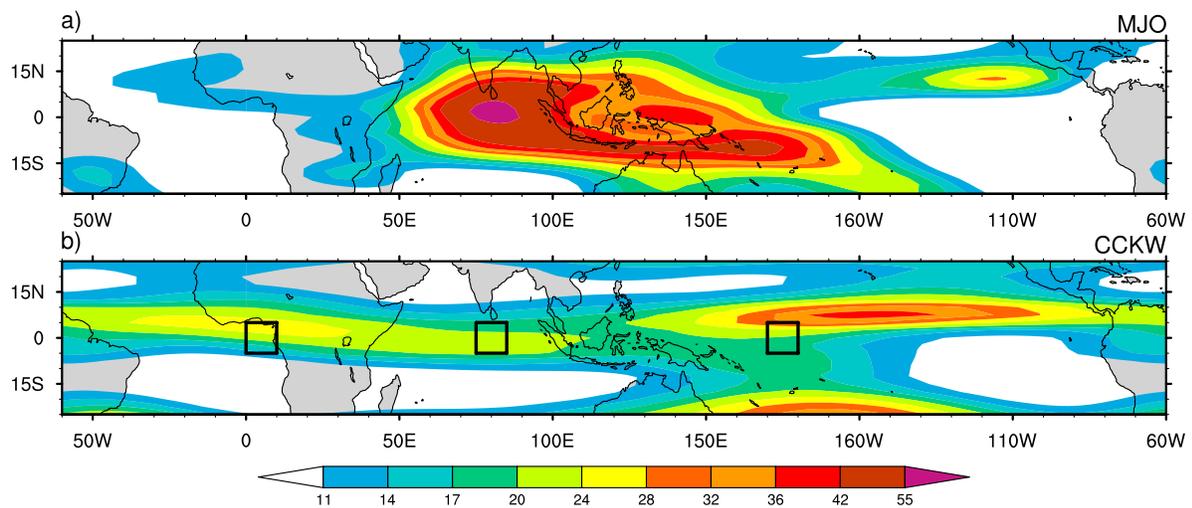
Figure 2. a) MJO and b) CCKW filtered OLR variance ($W^2 m^{-4}$) for the period 1979-2019. Three rectangular boxes represent the locations over which the MJO and CCKW indices were derived.
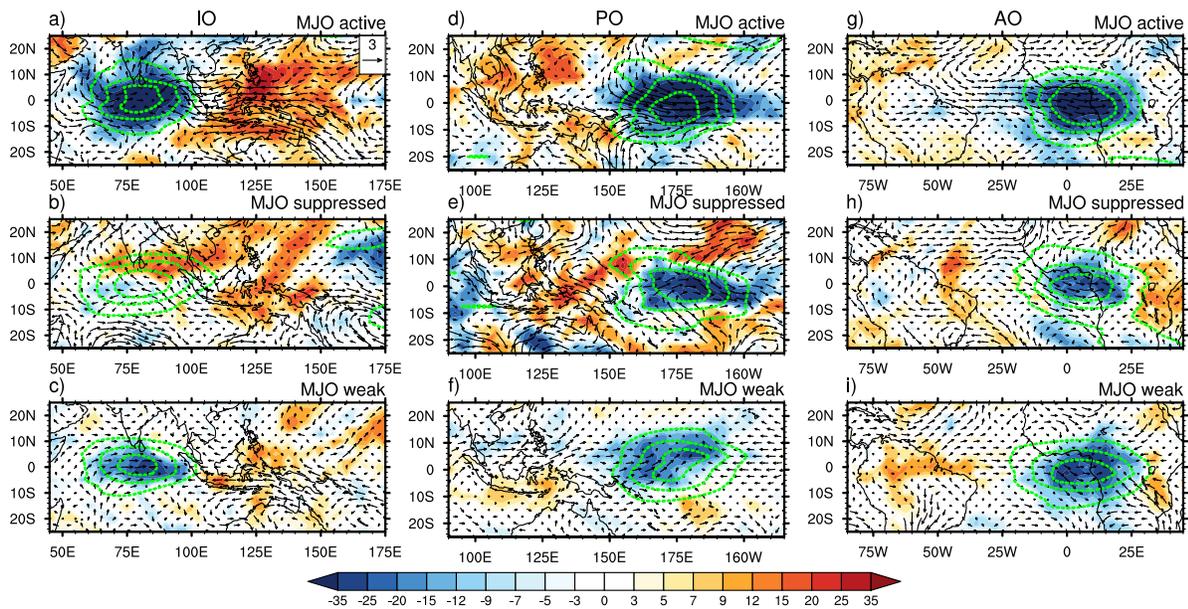
Figure 3. Composites of OLR (W/m²) and 850 hPa wind (ms⁻¹) anomalies calculated over the peak days of all CCKW events over the Indian Ocean (a-c), Pacific Ocean (d-f) and Atlantic Ocean (g-i) when the MJO is convectively active (a,d, g), convectively suppressed (b,e,h) and when the MJO amplitude is weak (c,f,i). Composites of CCKW filtered OLR (W/m²) anomalies (green contour lines representing -2.5, -5, -7.5 W/m²) are overlaid to highlight the location of CCKW convective region.
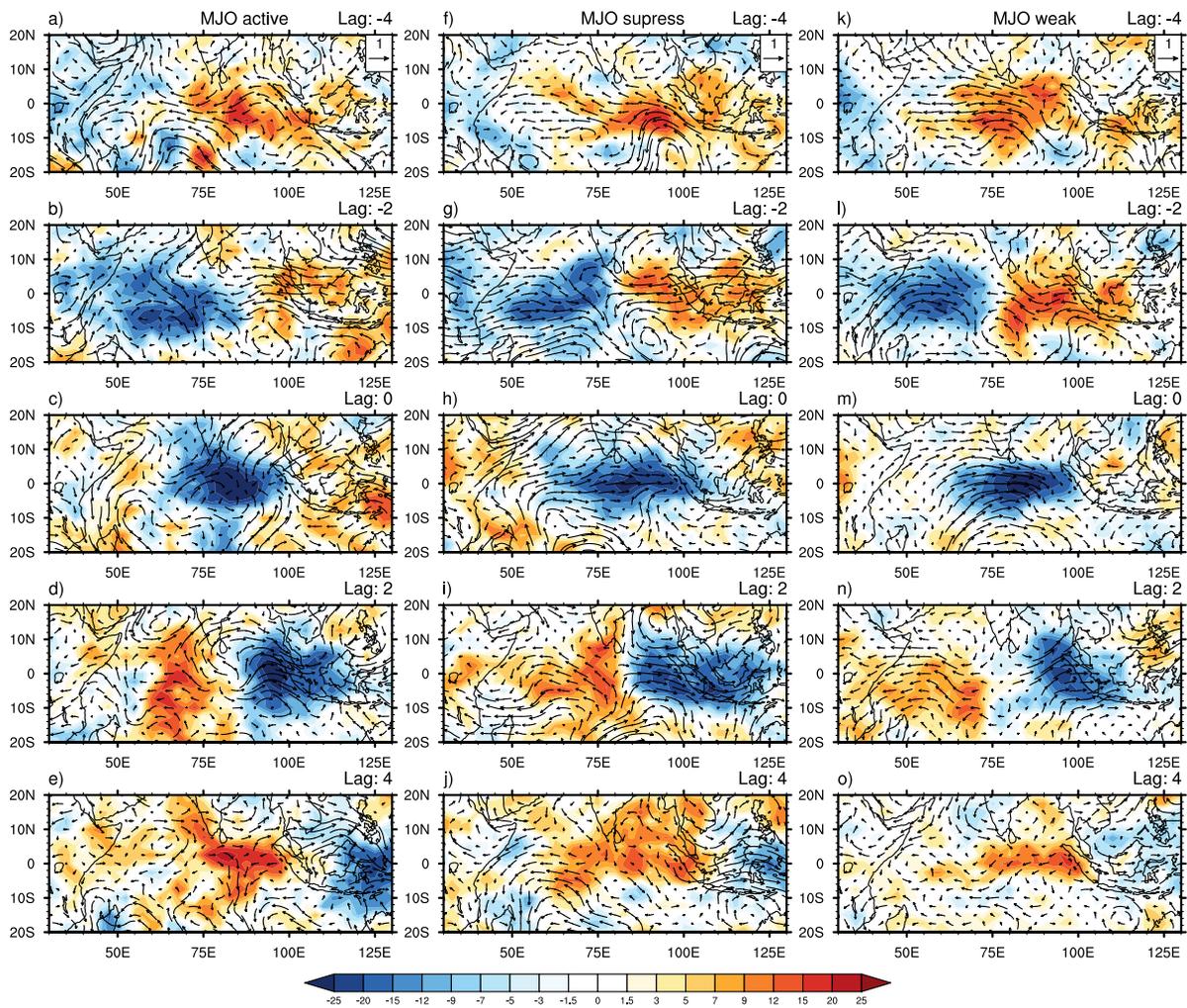
Figure 4. Lead-lag composites of CCKW events over the Indian Ocean domain, constructed using 3-20 day filtered OLR (W/m^2) and 850 hPa wind (m/s) anomalies when the MJO is convectively active (a-e), MJO is convectively suppressed(f-g) and MJO amplitude is weak (k-o). Positive/negative lag day represents number of days after/before peak of CCKW convection. Lag (in days) are shown on the upper right-hand corner.
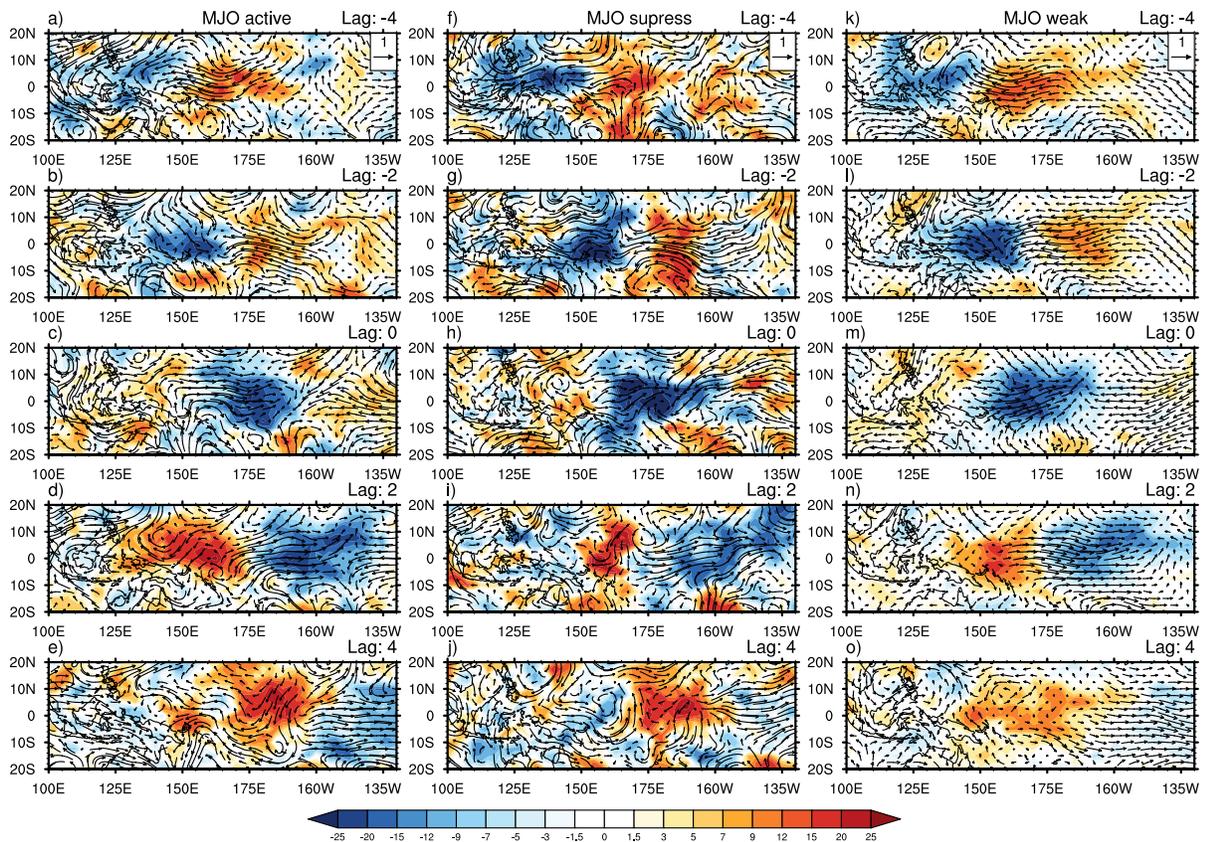
Figure 5. Same as figure 5 but for CCKW events over the Pacific Ocean domain.
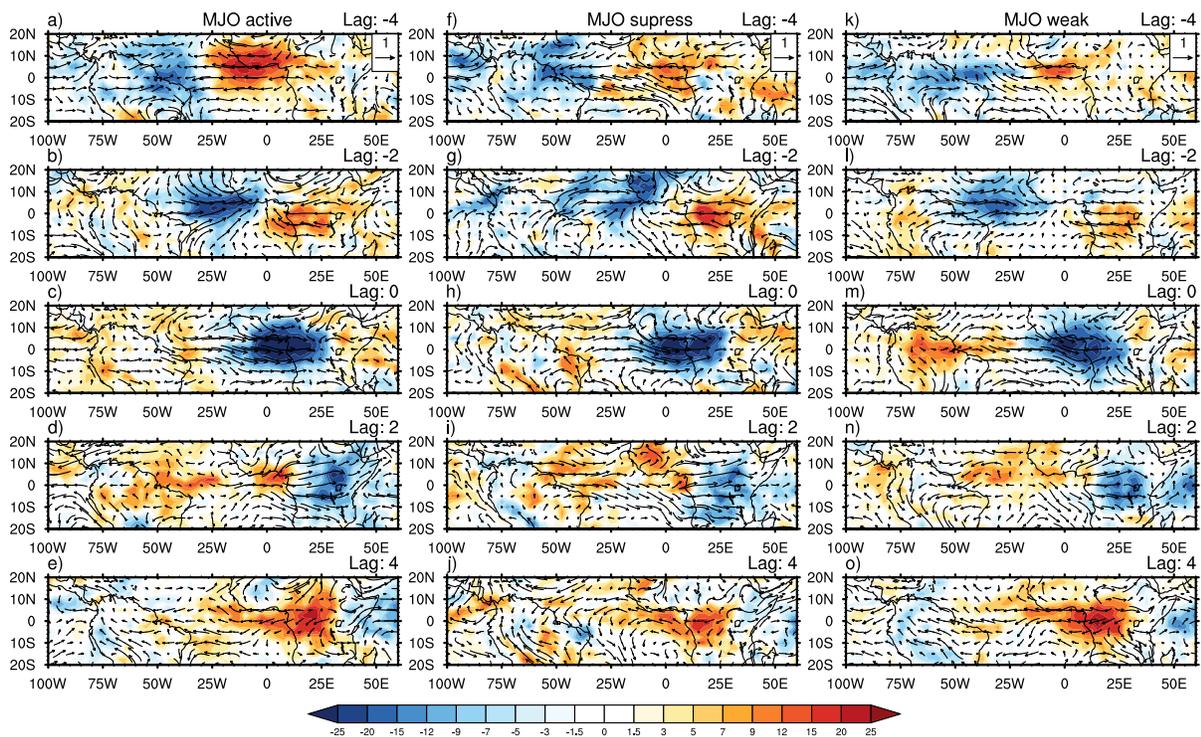
Figure 6. Same as figure 5 but for CCKW events over the Atlantic Ocean domain.
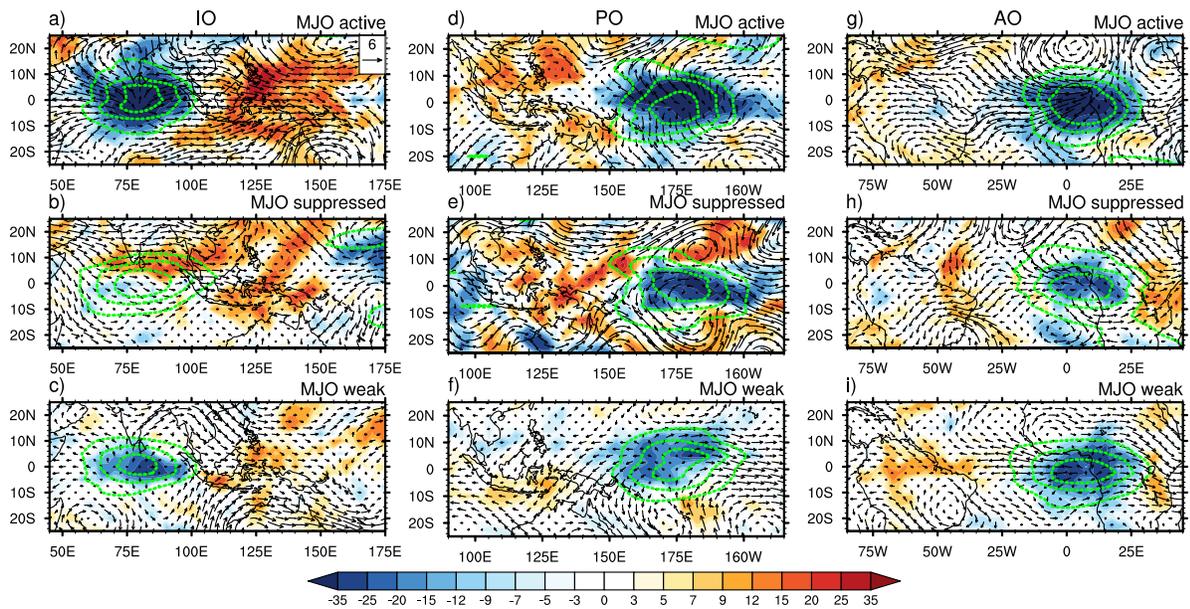
Figure 7. Same as figure 4 but wind anomalies at 850 hPa is replaced with the same at 200 hPa.
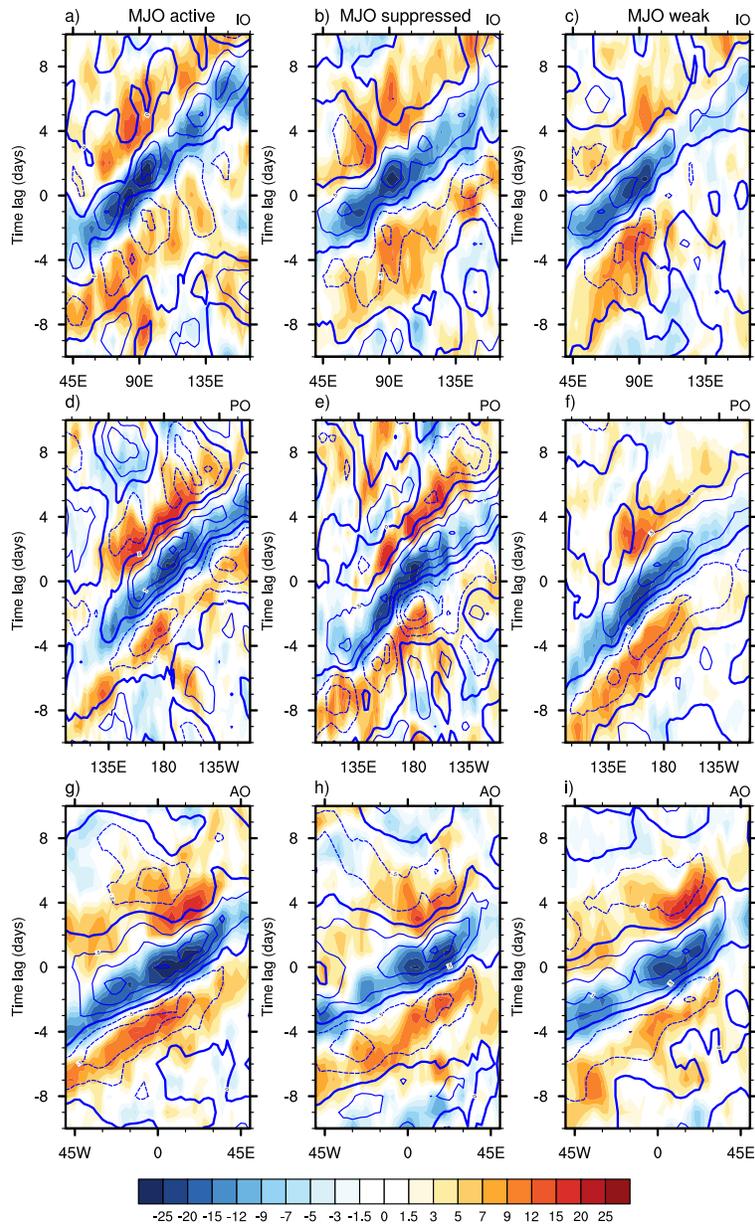
Figure 8. Phase propagation of CCKW events in OLR (W/m^2) and 850 hPa zonal wind (m/s) anomalies over the Indian Ocean(a-c), Pacific Ocean(d-f) and Atlantic Ocean (g-i) domains when the MJO was convectively active (a,d,g), when the MJO was convectively suppressed (b,e,h) and when the MJO amplitude was weak (c,f,i). The composite CCKW phase propagation was estimated by averaging the lead-lag composites in Figure 5-7 over latitudes 5°S-5°N.
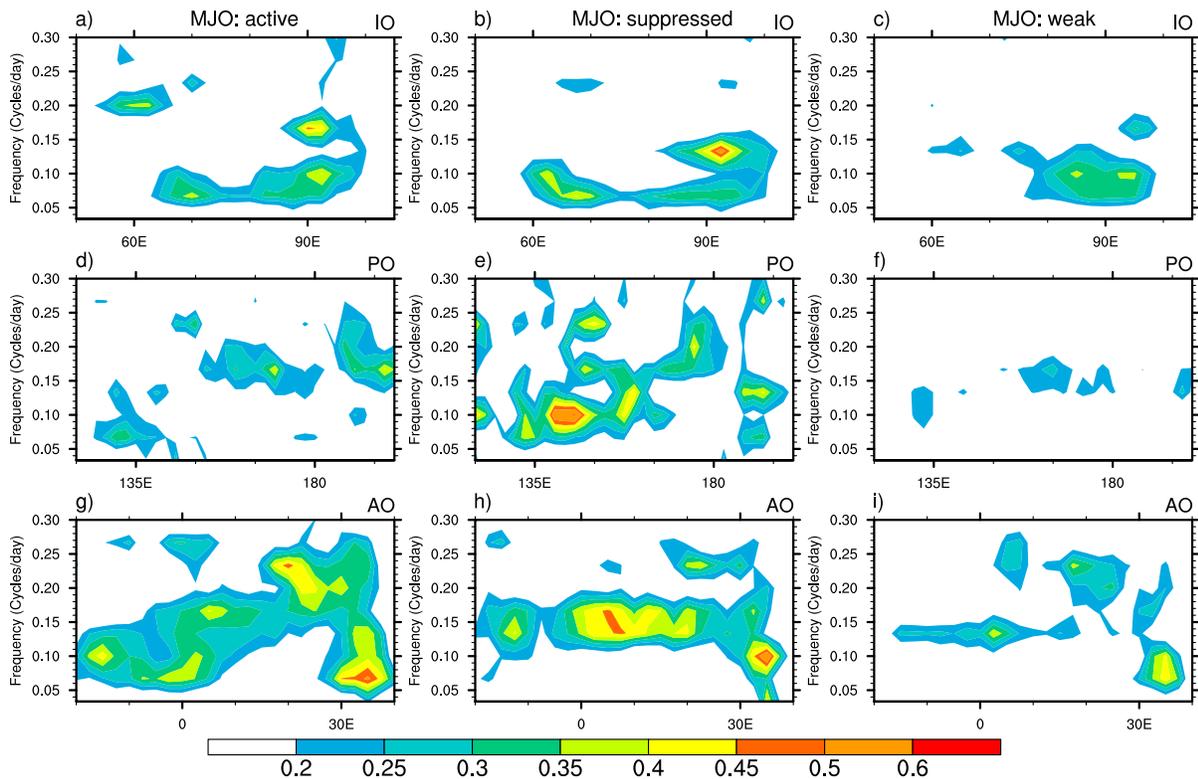
Figure 9. Composite coherence squared spectra between OLR and 850 hPa zonal wind anomalies estimated for CCKW events that occurred when the MJO was convectively active (a,d,g), MJO was convectively suppressed (b,e,h) and MJO amplitude was weak (c,f,i) over the Indian Ocean (a-c), Pacific Ocean (d-f) and Atlantic Ocean (g-i) domains. Composite coherence squared spectra was estimated by averaging the coherence squared spectra over all the events in each category and averaging symmetric with respect to the equator between 5°S and 5°N. Shaded regions are statistically significant at 99% confidence level.
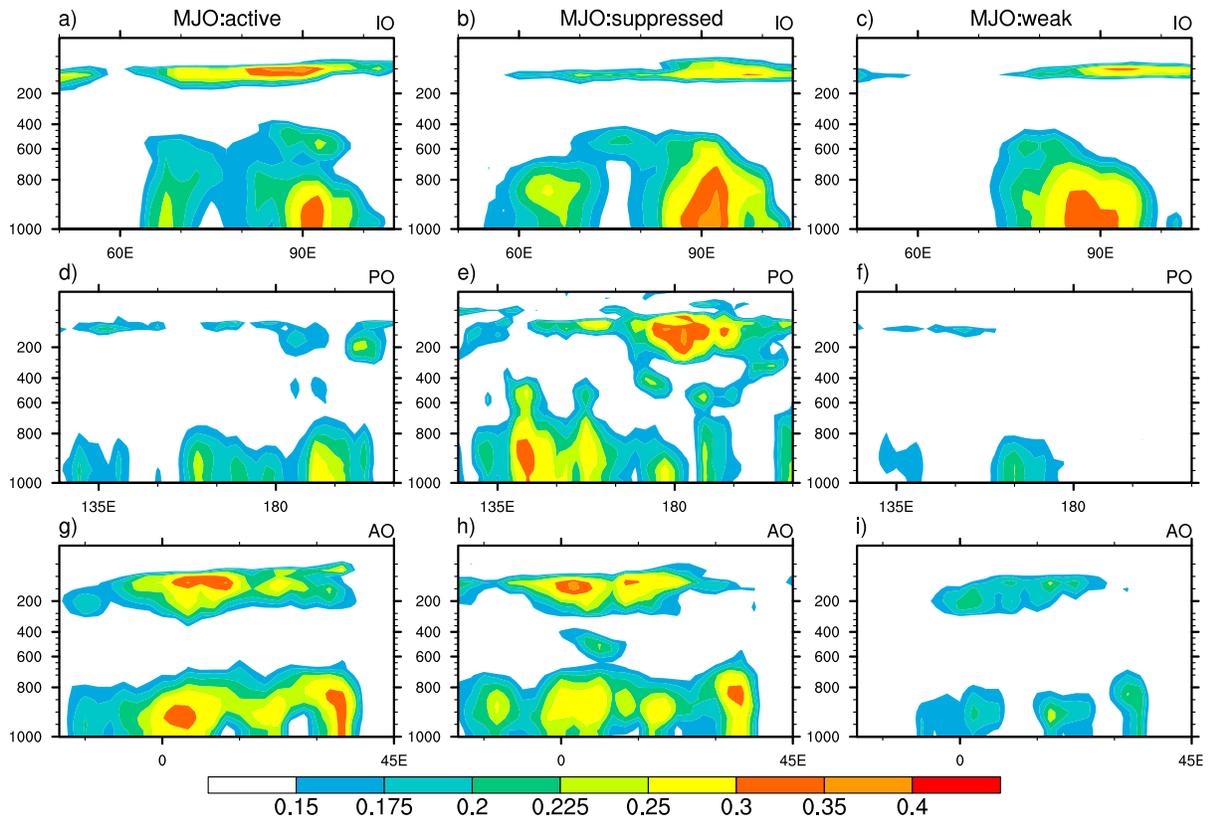
Figure 10. Pressure-longitude coherence squared spectra between OLR and 850 hPa zonal wind anomalies averaged over CCKW time scales estimated for all CCKW events when the MJO was convectively active, MJO was convectively suppressed and MJO amplitude weak over the Indian Ocean (a-c), Pacific Ocean (d-f) and Atlantic Ocean (g-i) domains. Shaded regions are statistically significant at 99% confidence level.
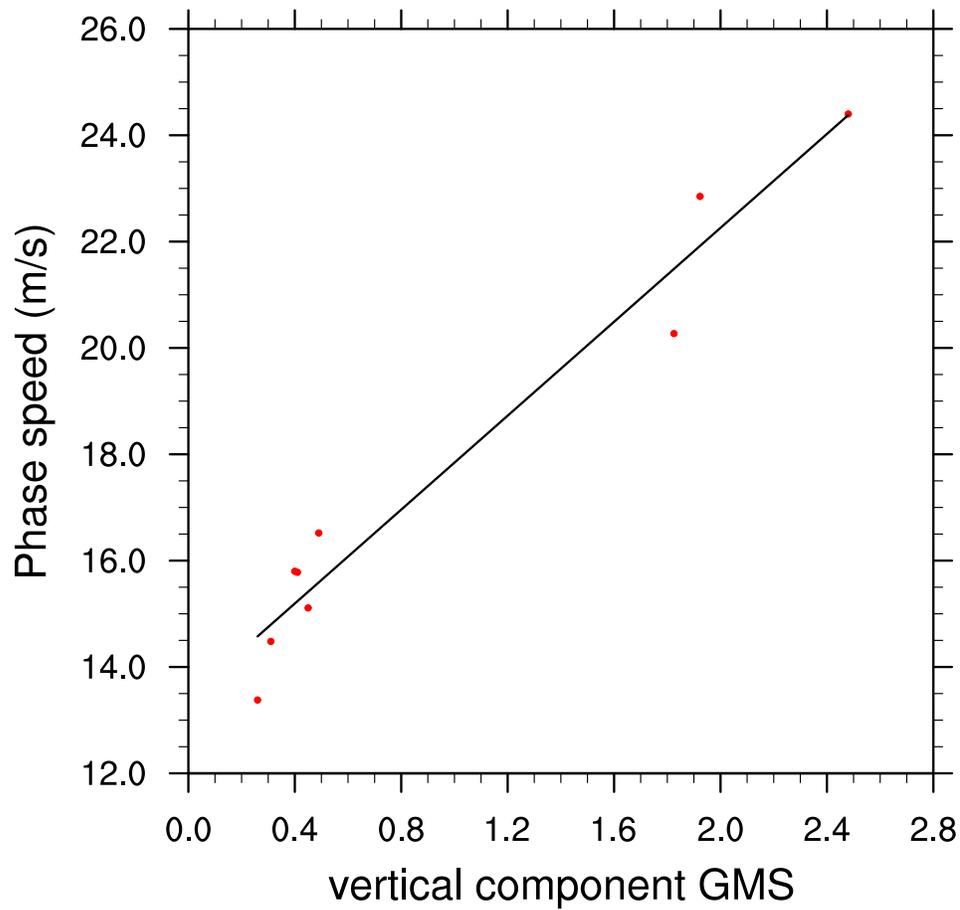
Figure 11. The relationship between the vertical component of normalized gross moist stability and CCKW phase speeds (ms^{-1}) over the Indian, Pacific and Atlantic Ocean domains for MJO convectively active, convection suppressed and weak amplitude states. Black line represents the least-square fit.
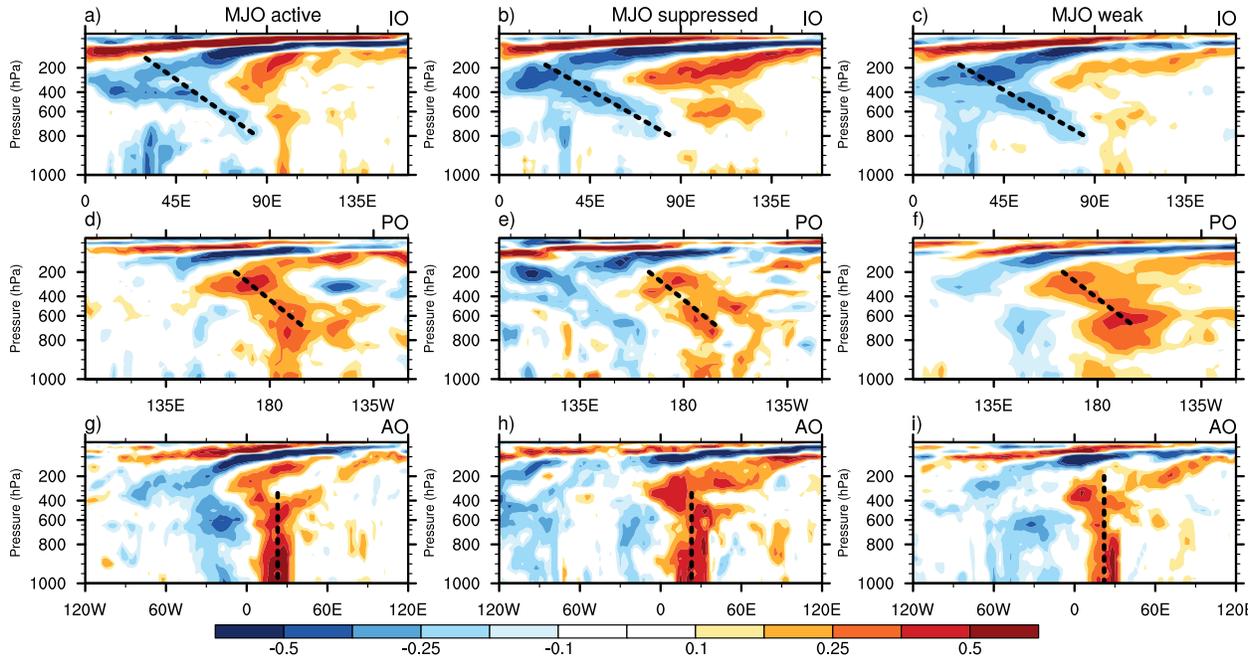
Figure 12. Pressure-longitude distribution of 3-20 day bandpass filtered temperature anomalies (K) averaged for all CCKW events when the MJO was convectively active (first column), MJO was convectively suppressed (2nd column) and MJO amplitude was weak (3rd column) over the Indian Ocean (a-c), Pacific Ocean (d-f) and Atlantic Ocean (g-i) domains. Dashed black lines are indicative of the tilt in the CCKW vertical structure in the troposphere.